UDC 532.592

# SOLITARY WAVE DYNAMICS AND VORTEX FIELDS NEAR SUBMERGED SLOTTED BARRIERS

I. M. Gorban<sup>†</sup>, A. S. Korolova, V. A. Voskoboinick, V. M. Vovk

Institute of Hydromechanics of NAS of Ukraine 8/4, Marii Kapnist Str., 03057, Kyiv, Ukraine †E-mail: ivgorban@gmail.com

#### Received 18.07.2024

Protecting coastal areas employing artificial structures is an important issue for the coastal engineering community. This study proposes a submerged, vertical, bottommounted screen with horizontal slots for reducing wave energy. When an incident wave encounters such an obstacle, it splits into transmitted and reflected waves. In addition, part of the wave energy is converted into kinetic energy of the vortex field due to flow separation from the structure walls. The study is focused on evaluating the hydraulic performance of this breakwater in terms of wave reflection and transmission coefficients. Circulation processes around the structure are also considered for deriving information about the directions and intensity of water exchange flows and bottom erosion. The problem is analyzed in the vertical plane, where the structure is considered a slotted barrier. It is assumed that the barrier comprises three impermeable elements and takes one of two possible configurations when its lower element either lies on the bottom or there is a gap between this element and the seabed. To identify the most suitable design, a numerical investigation of solitary wave interaction with slotted barriers of various shapes and porosity is carried out. The developed numerical procedure combines the boundary integral equation method used to determine free surface deformations and the hybrid vortex scheme for simulating the vortex field generated by the wave. The validity of the methodology is checked by the experimental research in the hydrodynamic tank of the Institute of Hydromechanics and by comparison with the data from other studies available in the literature. The solitary wave of non-dimensional amplitude  $A_i/h = 0.2$  is examined for the entire numerical experiment. Analysis of the free-surface evolution, as well as energy transmission and reflection coefficients, revealed that the protective properties of the structure deteriorate with increasing barrier porosity. In addition, permeability has a greater effect on high and narrow barriers than on lower and wider ones. Analysis of the vortex field created by the solitary wave around the slotted barrier revealed an intricate flow pattern on the leeward side. This pattern consists of two pairs of large-scale counter vortices, whose interaction forms downward and upward water flows along the structure. These vortices push the liquid through the gaps to the windward side, establishing reverse flows between the close zone and the open sea. This is a reason for the increase in water exchange intensity several times between different sides of the structure compared to an impermeable barrier. The data obtained infer that a slotted barrier of porosity (0.2...0.3) will be the most successful among structures of this type, both for shore protection and sustaining the health of the coastal ecology.

KEY WORDS: solitary wave, submerged breakwater, horizontally-slotted barrier, method of boundary integral equations, vortex method

#### 1. INTRODUCTION

The development and rational use of coastal areas is an important source of income for many coastal countries. The safe functioning of infrastructure in maritime regions requires its protection from the destructive energy of surface waves. In recent years, active coastal protection structures, such as submerged breakwaters, have been increasingly used. They are installed on the seabed parallel to the shoreline and reduce wave energy due to a sudden drop in water depth. Traveling over a submerged obstacle, the incident wave splits into transmitted and reflected waves. In addition, part of the wave energy is converted into kinetic energy of the vortex field due to the separation of the flow from the walls of the structure. The design of a submerged breakwater has traditionally taken into account wave transmission, but to create a modern protective structure, coastal engineers must consider care for the environment along with its effectiveness against waves. Rubble mounds and gravity-type breakwaters require a great amount of construction material and a high capacity of the seabed. In addition, they block water in the coastal zone, which leads to a deterioration in its quality. To overcome these disadvantages, thin structures in the form of rigid, pile-supported vertical screens have been proposed and examined [1–3].

In practice, permeable screens are mainly used owing to their low cost, lower impact on dynamic loads, and ability to support exchange processes between the open sea and the sheltered area. The elements of a permeable screen can be installed either horizontally or vertically, and, thus, the problem to be solved results in two-dimensional and threedimensional setups for horizontal and vertical slots, respectively. In this study, we consider a horizontally slotted screen, which is a permeable barrier in the vertical plane. The operation of similar breakwaters has given rise a large number of experimental and theoretical studies that substantiated their effective design. Early on, surface-piercing barriers in the field of regular waves were mainly considered (e.g. [1,4,5]). The emphasis was on the study of the hydraulic performance of the breakwater in terms of transmission and reflection coefficients. In [6], the barrier with impermeable surface-piercing upper part and slotted lower part was analyzed under the action of normal regular waves. The effect of both wavelength and structural parameters on the transmission and reflection coefficients was investigated using a specially developed theoretical model. It was shown that with the correct selection of the ratio between the impenetrable part and the gap of the barrier, the energy of the incident wave can be reduced by 50%.

The progress in the study of slotted breakwaters including wave screens is reviewed in [7]. Although the authors paid more attention to surface-piercing-type barriers than submerged ones, they emphasized that the latter have potential engineering applications for mitigating tsunami hazards and reducing shoreline erosion. It was also pointed out that the energy dissipation associated with the vortex shedding at a slotted submerged wall needs to be considered in order to adequately assess its ability for shore protection.

Long waves, such as tsunamis or storm surges, are the most dangerous for coastal areas. To describe their evolution in the surf zone, the solitary wave model is often used, as it is a limiting condition for the run-up of an extreme non-linear long wave [8]. The connection of a solitary solution with ocean waves also consists in the fact that periodic waves, when passing from deep water to shallow water, are unstable and break up into groups whose circumferential line has the properties of a soliton. One of the early theoretical studies of the propagation of a solitary wave over an uneven bottom is paper [9]. The method of characteristics was applied there to show the disintegration of the incident solitary wave into a wave chain. The results obtained were confirmed by experimental data in the wave channel. Researches of solitary wave dynamics over submerged obstacles were continued using asymptotic methods developed within the framework of the shallow water model. [10, 11]. Significant progress in explaining the evolution of surface waves has been achieved based on the Boussinesq equation. To expand the range of applicability of this theory to deep water, an additional term is introduced into the equation, which improves its dispersion characteristics [12]. Further efforts of the researchers are aimed at developing stable numerical schemes (solvers) for Boussinesq-type equations, as well as at studying the transformation and breaking of waves that interact with both submerged obstacles and a sloping shore (e.g. [13–15]).

The progress in computer technologies has made it possible to more finely simulate the hydrodynamic processes that develop during the interaction of a solitary wave with an uneven bottom, in particular, taking into account the shape and size of submerged obstacles. The boundary element method (BEM), which is based on the potential flow theory, is a commonly adopted numerical technique that provides accurate results over a wide range of wave amplitude. In particular, the interaction of a solitary wave with a submerged semicircular cylinder was described in a wide range of both the wave height and the cylinder radius [16]. In the paper [17], the BEM was applied to study the wave breaking over submerged obstacles of various configurations. A new application of the potential theory to the simulation of wave evolution is presented in [18], where the interaction of a solitary wave with a wave energy converter was simulated in the presence of bottom irregularities and collinear currents.

Although the potential flow theory ensures good modeling of free surface dynamics, it is unable to describe the generation of a vortex field near an uneven bottom. At the same time, a solitary wave is known to be similar to a local uniform flow. When the wave approaches a bottom irregularity, the processes develop that usually accompany the modification of flow in a viscous fluid, including the appearance of a negative pressure gradient along the solid boundary, the development of a shear flow, and the generation of a vortex field. To take into account the above effects, the numerical algorithms based on the viscous flow equations should be employed. The volume of fluid (VOF) and mark-and-cell chart (MAC) methods are two main techniques used for modeling viscous fluid flows with strong nonlinearity on a free surface [19–21]. They are based on the averaged Navier–Stokes equations (RANS) supplemented by a  $k-\varepsilon$  nonlinear turbulence closure model. With the use of this approach, significant advances have been made in understanding the phenomena that accompany the passage of solitary waves over submerged obstacles. In [22], the interaction of a solitary wave with a submerged rectangle was investigated. It is argued that the contribution of viscous effects to the dissipation of wave energy can reach 15%. Paper [23] focuses on investigating the drag of a rectangular dike caused by a solitary wave. The pressure drag is shown to be much greater than the friction drag, although the induced local shear stress on the top surface of the dike can be quite large. The interaction between a solitary wave and a submerged vertical bottom-mounted barrier is investigated in [24]. Both the wave transformation and the dynamics of the vortex field generated near the obstacle are described in detail for breaking and non-breaking waves. The effectiveness of the barrier against waves is estimated by evaluating the wave RTD coefficients using the energy integral method.

Despite the obvious fact that traditional CFD methods have yielded important results in wave dynamics, their use is associated with serious technical challenges. These are related to the difficulties in tracking the fluid interface and implementation of the free surface boundary conditions, especially when a moving grid is used. A needed alternative has been found in the development of mesh-free methods based on the Lagrangian representation of the flow field. These include the Smoothed Particle Hydrodynamics (SPH) [25] and Moving Particle Semi-implicit (MPS) method [26], which employ particles moving according to governing dynamics. In [27], the vortex fields generated by a solitary wave passing over submerged rectangles of various widths and heights were investigated in detail using SPH. The study, the results of which are presented in [28], concerns the interaction of the solitary wave with the composite submerged breakwater combining a quarter circle and a square. Among other things, it was obtained that the depth of the submerged breakwater has a significant influence on wave dissipation. Both the MPS method and its application to the analysis of tsunami-structure interaction are represented in [29].

In [30], a numerical scheme was developed that combines the boundary integral method and the vortex method to study wave-structure interaction in viscous fluid. In accordance with it, the generation of vorticity by the free surface is predominantly neglected and the vortex field is formed exclusively due to the separation of the boundary layer from the walls of a submerged structure. Given the fact that the considered problem is characterized by a sufficiently large Reynolds number, such an approach is justified, especially since it is confirmed by the good agreement between the results of calculations and the data of laboratory experiments. The results of the paper [31] suggest that the vortex field is the main factor determining the drag of an underwater structure under the action of a solitary wave. A similar numerical scheme was applied in [32] to simulate the propagation of a solitary wave over a submerged barrier. Two types of wave-barrier interaction were identified there. There is a weak interaction when the incident wave splits smoothly into the reflected and transmitted solitons and a strong interaction when the wave breaks down. It was found that the fate of a solitary wave over a barrier depends on the interaction coefficient, which is the ratio of the wave amplitude to the thickness of the water column above the obstacle. The critical value of the interaction coefficient at which these modes switch was estimated to be approximately 1.

A slotted breakwater can contribute to greater wave energy dissipation due to flow separation from its elements. Therefore, the impact of such structures on wave dynamics can be correctly estimated either by experimental methods or by utilizing numerical schemes that take into account viscous effects generated by the wave. Partially submerged rigid curtain walls in the shape of a vertical barrier in cross-section are one of the successful implementations of permeable breakwaters, where water passes through an opening between the wall and the seabed. The most comprehensive study of the interaction of solitary wave with a vertical surface-piercing barrier is presented in [33]. The characteristics of the transmitted and reflected waves, as well as the velocity fields and wave-induced structural loads, were

found experimentally and numerically over a wide range of problem parameters, such as water depth, incident wave amplitude, and draught of the barrier. A laboratory experiment was conducted to obtain data for validation of the numerical model based on the Reynolds-averaged Navier–Stokes (RANS) equations and the k- $\varepsilon$  turbulence closure model. Numerical calculations ensured an array of results for deriving generalized formulae for maximum runup height and maximum wave force. In [34], the Smoothed Particle Hydrodynamics (SPH) was used to calculate non-linear, dispersive reflection and transmission characteristics of the solitary wave interacting with a partially immersed screen. The effect of both the wave height and the draught of the curtain wall on the protective characteristics of the structure is analyzed. The research stated that the partially immersed curtain breakwater is effective in dissipating incoming wave energy if its immersion depth is over half of the water depth. In [35], the wave-curtain screen interaction is investigated with the help of the Weakly Compressible Smoothed Particle Hydrodynamics (WCSPH). The submergence depth of the screen is shown to play a crucial role in its performance as a breakwater.

The propagation of a solitary wave over a fully submerged vertical slotted barrier was studied in [36, 37] using a laboratory experiment and numerical simulation. The wave-structure interaction is detailed in terms of free surface elevation, velocity, and turbulence characteristics. Flow visualization revealed the development of a complex vortical pattern near the slotted barrier due to the interaction of vortices shedding from each element of the structure. In this case, the vortex field is a potential scouring factor for a bed. The authors pointed out that the gap between the elements and the water depth are critical parameters that affect the vortex dynamics near a slotted barrier.

The importance and complexity of the problem under consideration necessitate the development of new methods to supplement our knowledge of the interaction of waves and underwater obstacles. In this study, the hydraulic performance of submerged horizontally slotted barriers against long waves is numerically estimated on the base of the Lagrangian representation of the flow field. The developed calculation methodology consists of two components. The first is associated with the free surface, and the second identifies the vortex field generated by the wave. In the task setting, the effects of viscosity and vorticity generation at the free surface are ignored, as well as the flow field far from the structure is supposed to be irrotational. These assumptions permit to application of the potential-flow analysis in calculating the free surface evolution. The viscous flow under the free surface is modeled with the use of the hybrid vortex method developed in [38], which is based on the velocityvorticity form of the Navier-Stokes equations. It should be noted that the two components are not solved independently because they affect each other. The difference between this algorithm and the previous analogous methods lies in the simpler involvement of the free surface dynamic condition, which, nevertheless, does not affect the calculation results. To verify the numerical algorithm, a set of laboratory experiments in the hydrodynamic flume was performed with a solitary wave passing above an impermeable vertical barrier. The free surface elevations at the same locations were measured in the numerical simulation and the experiment and a good match was found both for reflected and transmitted waves. The numerical calculations were then carried out over a wide range of slotted barrier permeability to derive wave energy coefficients as well as to discuss the free surface evolution, vortex shedding, and water exchange flows around the structure.

## 2. PROBLEM STATEMENT AND NUMERICAL MODEL

The mathematical statement of the problem under consideration is based on two assumptions, namely, that a solitary wave propagates perpendicular to the submerged obstacle, and the elements of the slotted barrier are installed horizontally. This allows us to consider the developing processes in a vertical section, which implies a two-dimensional (2D) problem. It is assumed that the wave propagates in a two-dimensional numerical channel with a submerged slotted barrier at the floor (Fig. 1). A Cartesian coordinate system is fixed in such a way that its origin is connected with the midpoint of the barrier, the x-axis lies in the bottom and the y-axis points vertically upward. The still water depth is h and the amplitude of the incident wave is  $A_i$ . The height and length of the barrier are depicted by d and a respectively. The structure permeability is characterized by the porosity p, defined as the ratio p = s/(s+b), where b is the length of the impermeable element and s is the gap space. Two configurations of the barrier are evaluated when its lower element either lies on the bottom or there is a gap between this element and the bottom (see Fig. 1).

Under the assumption that the fluid in the numerical channel is incompressible with constant density and viscosity, its motion is governed by the continuity equation and the Navier—Stokes equations, the right side of which includes the gravitational force and the viscous force. The problem statement consists of the no-slip condition both on the channel bed and the impermeable elements of the barrier as well as the zero-stress condition at the free surface. The latter consists of the kinematic condition, which states that there is no flow across the interface, and the dynamic condition declaring the continuity of stresses when passing across a free surface. Note that the surface tension effect is not considered. One can find a detailed description of the mathematical model in [39]. To avoid wave reflection at the lateral boundaries of the numerical wave flume, wave damping is introduced following the method proposed in [40]. For this reason, numerical sponge layers are put at both lateral boundaries to absorb the outward-traveling waves.

The problem is solved in a dimensionless form when the variables are scaled by the still water depth h and the phase speed of linear long wave  $\sqrt{gh}$ , where g is the gravity acceleration;  $\bar{t} = t\sqrt{g/h}$  is the dimensionless time (further the overline will be omitted). The Reynolds number is evaluated based on the depth-averaged velocity under the wave crest  $U = (A_i/h)c$ , where  $c = \sqrt{g(h+A_i)}$  is the wave celerity, then  $\text{Re} = Uh/\nu = A_i\sqrt{g}(h+A_i)/\nu$ . The Froude number is introduced as  $\text{Fr} = c/\sqrt{gh}$ .

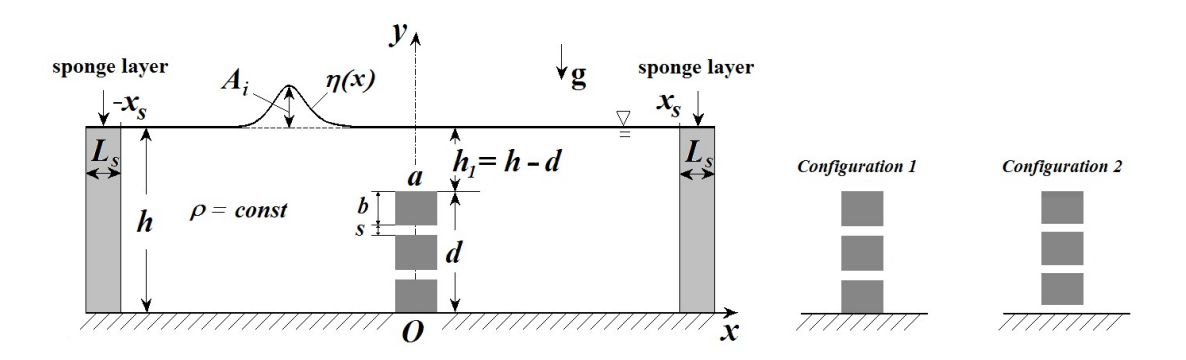


Fig. 1. Schematic diagram of the problem (left) and slotted barrier configurations (right)

The boundary value problem is solved under the assumption that the flow close to the free surface is irrotational and vorticity is only created at the solid walls, namely the channel bottom and the submerged barrier. A boundary integral-equation method is applied to obtain free-surface elevations and a vortex method is used for simulation of viscous effects. It should be noted that viscous and irrotational calculations are interrelated in the sense that they take into account the mutual influence of these two components of the flow field. The developed algorithm is described in detail in [32,39], so only its main features are considered here. This technique is based on the Lagrangian representation of the flow field and follows the scheme outlined in [30], except for some points.

The boundary integral method is a well-known technique that has long been used to model the interface (e.g. [40,41]). In the flow under consideration, both the free surface and the walls of the submerged barrier are represented by the vortex sheets, whose intensity is determined by the boundary conditions. To take into account the influence of the channel bottom, the fundamental solution of the Laplace equation for a point vortex in a half-plane is used [42]. This allows us to fulfill automatically the no-penetration condition at the bottom. The discrete scheme is constructed in such a way that continuous vortex sheets are replaced by sets of straight segments (panels) of equal length with a piecewise distribution of the vortex strength. Further, each segment is compressed into a discrete vortex located in the middle. With this choice, the integrals included in this model are approximated by sums based on trapezoidal quadrature.

To solve the problem, it is necessary to calculate at each time instance the strengths of the discrete vortices distributed along the free surface and the barrier, as well as the positions of the points on the free surface. The dynamic boundary condition on the free surface and the impermeability condition at the barrier are used to construct a linear algebraic system regarding the vortex strength. Note that the part of the system that deals with the free surface is written based on Bernoulli's law and on the known fact that the tangential velocity experiences a discontinuity when passing through a vortex layer [39].

To integrate the evolution equation with respect to the coordinates of the free-surface points, the fourth-order Adams–Bashforth–Moulton (ABM) predictor-corrector scheme is used. It should be taken into account that problems with a free surface are essentially singular; as a result, the accuracy of the integration is very sensitive to the small perturbations introduced by the numerical scheme. This requires maintaining a fine balance between the choice of parameters of the discrete scheme and the integration method. In addition, it is desirable to avoid large gradients of variables on the free surface, which can be achieved by applying regularization procedures. In this study, the elimination of extreme velocity gradients at the free surface is achieved by recalculating the length of the vortex panels so that they become the same at each time step. The intensity of the vortex layer is redistributed according to the new lengths of the segments. Note that the number of vortex panels on the free surface remains constant throughout the simulation.

The viscous flow field under the free surface is simulated via the vortex method, which uses the vorticity transport equation instead of the traditional pressure-velocity formulation of the Navier–Stokes equations [43]. The pressure field is eliminated from this equation, resulting in only the boundary condition containing the gravitational force. To solve the equation, we use the hybrid vortex scheme developed in [38]. It involves a Lagrangian framework for the advection process but it also handles a fixed grid, which facilitates the

prescription of the no-slip boundary conditions as well as the modeling of the diffusive term. In this investigation, the vertical size of the grid is not fixed, so the upper boundary of the computational domain is approximated by a step function, which is constructed at each time step. The vorticity flux into the fluid is determined through the strength of the vortex sheet distributed along the walls of the submerged obstacle. Note that the validity and efficiency of the used scheme have been confirmed when solving various two-dimensional problems of viscous fluid dynamics with solid boundaries [44, 45].

#### 3. RESULTS AND DISCUSSION

## 3.1. Setup of the numerical experiment and verification of the algorithm

The numerical wave flume used in this study is of 1 m depth and 140 m length. Normalized parameters of the problem will be further considered, so the dimensionless flume length is 140h. The absorbing layers' width adjoining the flume's lateral sides is put to 2h. The submerged obstacle is situated in the middle of the computational domain. At the initial time instant, the wave crest is located at x/h = -20, and then it propagates from left to right. To derive the initial data for a solitary wave, profile, and velocity potential, the MatLab implementation of the iterative method developed in [46] is utilized. Since the method computes an approximate solitary solution of the Euler equations, it allows for both horizontal and vertical motions of fluid particles beneath the wave. In this way, it is possible to model not only the evolution of the free surface but also the dynamics of the vortex field created by a solitary wave around a submerged structure. The number of vortex panels along the free surface is equal to  $N_{\Sigma} = 2800$ ; a uniform grid of resolution  $\Delta x = \Delta y = 0.01h$  is put on the flow field; the time step is  $\Delta t = 0.005 \sqrt{g/h}$ . The amplitude of the incident wave is taken  $A_i/h = 0.2$ . The Reynolds number calculated these depth and wave amplitude equals Re =  $0.69 \cdot 10^6$ . The slotted barriers of heights d/h = 0.8 and d/h = 0.9 are investigated. Porosity p is the main parameter whose influence on the hydraulic quality of the structure is studied. It lies in the range of p = 0.1 to 0.5, that is, the maximum total length of the slots can reach 50% of the height of the structure.

To check the validity of the numerical algorithm, the obtained results are compared with the data of our laboratory experiment as well as with analogous results known from other

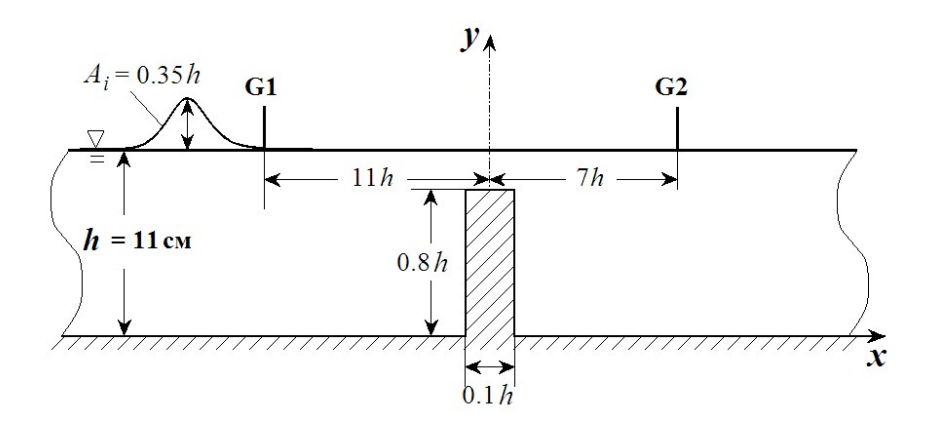
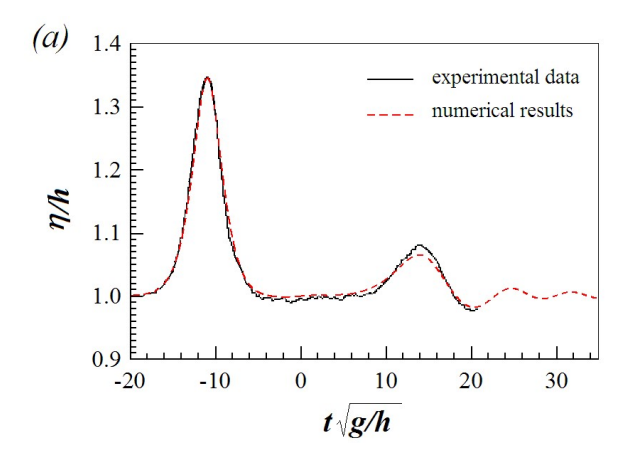


Fig. 2. Parameters of the problem in the experiment and calculations when investigating the interaction of a solitary wave with a submerged barrier



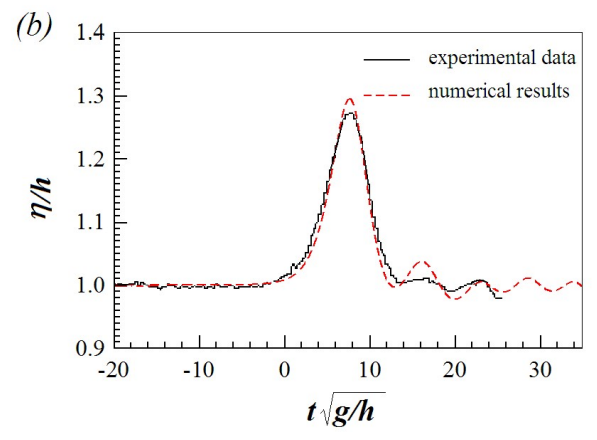


Fig. 3. Comparisons of the free surface elevations between experimental data (black line) and computational results (red line) at the gauge locations G1(left) and G2 (right)

studies available in the literature. The experiment was conducted in a glass-wall flume of the Institute of Hydromechanics. A solitary wave propagating above a thin non-permeable barrier was examined. The laboratory setup, equipment, and experimental technique are described in detail in [47]. Fig. 2 illustrates the normalized parameters of the problem under consideration, as well as the positions of the gauges, and recorded elevations of the free surface.

Fig. 3 demonstrates the time histories of instantaneous free surface elevations  $\eta(t)$  at the locations G1 and G2 derived in the measurements (solid black lines) and the calculations (dotted red lines).

The comparison indicates that the numerical calculations fit the measurements well for the main waveforms in terms of the incident and reflected waves recorded by gauge G1 and the transmitted wave recorded by gauge G2. It should also be noted that the experimental and numerical results are in good agreement with respect to the propagation rate of free surface perturbations. Here and below, the dimensionless time t=0 is defined as the instant when the crest of a solitary wave passes exactly above the top of the obstacle.

The present numerical model was also tested with the classical example when a

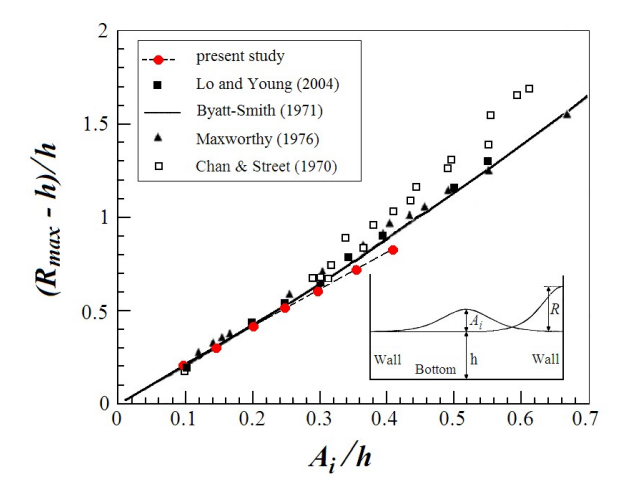


Fig. 4. Relative maximum run-up height against incident wave amplitude

solitary wave reflects from a solid vertical wall. It is the problem of a wave returning to its initial state after colliding with the wall. It has an approximate asymptotic solution [48] and has also been repeatedly studied in laboratory experiments (e.g. [49,50]), which provided data for testing numerical algorithms. The scheme of the problem and the primary parameters are depicted in the lower part of Fig. 4. Calculations are carried out for initial wave amplitudes

from the range of  $A_i/h = 0.1$  to 0.4 with the step of 0.05. The dynamics of the wave looks this way: it grows when approaching the wall and reaches a maximum when hitting the wall. Fig. 4 shows the comparison of the calculated maximum run-up height with the analytical solution of Byatt-Smith [48], the experimental data of Chan and Street [49], Maxworthy [50] as well as with the numerical results of Lo and Yang [51]. It can be seen that the results of the present research are in good agreement with the data presented by previous investigators.

It should be also mentioned that the present numerical scheme has been applied to simulate the interaction of a solitary wave with a submerged step [39]. Analysis of the obtained results and their comparison with the data from [52] demonstrated that the calculations accurately predict the fission process and the dependence of the number of secondary solitons on both the amplitude of the incident wave and the step height.

## 3.2. Wave evolution and energy coefficients

The key information about the hydraulic advantages of the slotted barrier as a breakwater can be derived by studying the fission of the incident wave into transmitted and reflected waves and then estimating the energy of these waves. Fig. 5 illustrates the evolution of

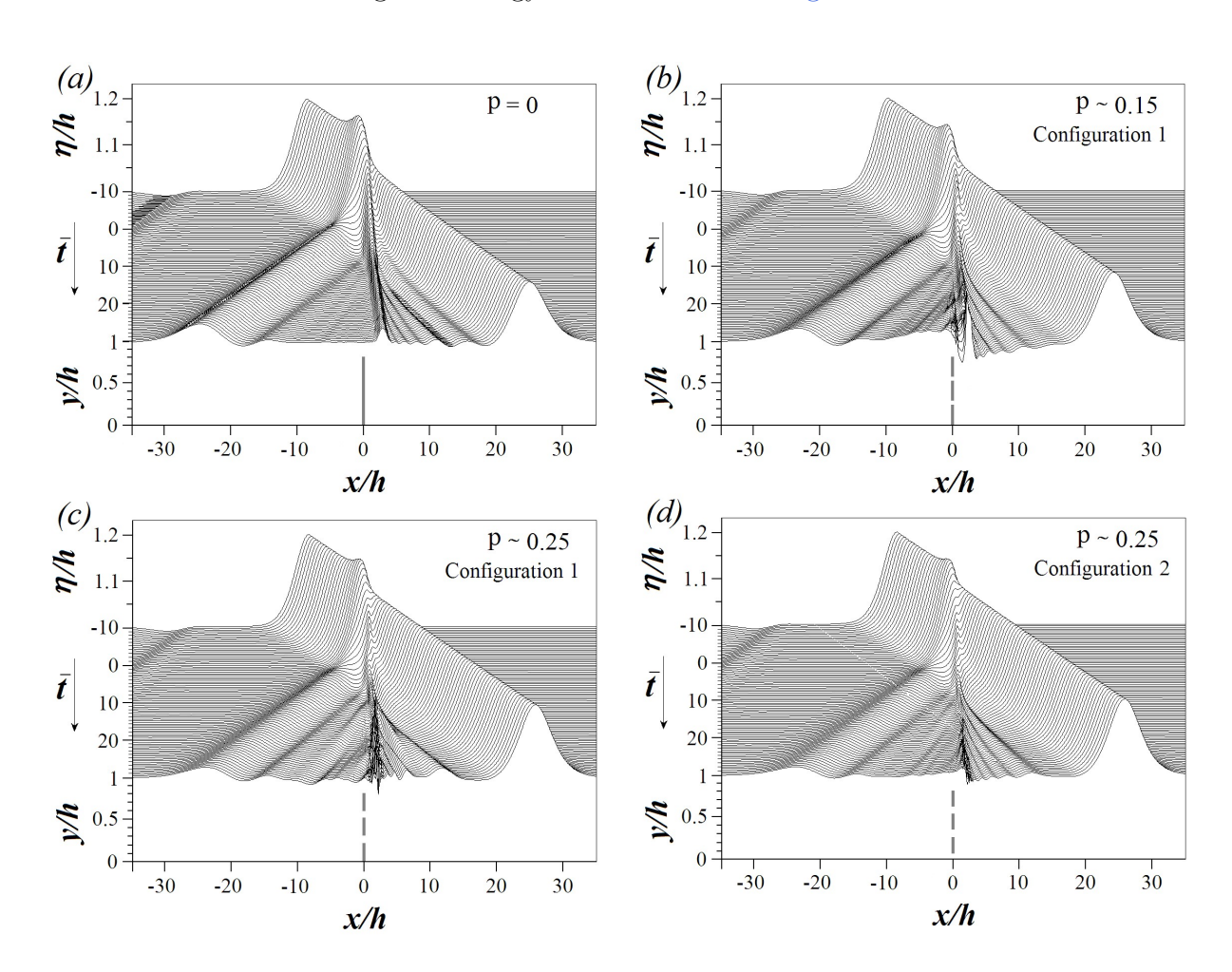


Fig. 5. The influence of barrier porosity on the free-surface evolution for the solitary wave interacting with the slotted barrier

the wave profiles when the soliton of relative amplitude  $A_i/h = 0.2$  passes over submerged barriers of different porosity. The development of the free-surface elevation with time is here depicted with the time step of  $50\Delta t$ . The barrier height and length are d/h = 0.8 and a/h = 0.1 respectively. The pictures are arranged in order of increasing porosity. Fig. 5a deals with the solitary wave passing over an impenetrable barrier, when p = 0, so it reflects the classical pattern of interaction of a solitary wave with an underwater obstacle. It can be seen that the incident wave grows as it approaches the obstacle, and then splits into a reflected wave and a transmitted wave, which propagate in opposite directions. The process is complicated due to the fission of the transmitted wave into a chain of secondary solitons. In addition, there is a local rise of the free surface just behind the obstacle produced by the intense recirculation flow. Note that the free surface remains regular throughout the process.

In the following pictures, the porous effects are taken into account. The slotted barrier in Fig. 5b is of Configuration 1 with narrow gaps between the solid sections, so that p = 0.15. In this case, the wave-structure interaction is characterized by the appearance of well-defined stochastic disturbances of the free surface above the barrier. As a result, the free surface in front of the obstacle rises and falls behind it. The dispersive tail of solitons behind the transmitted wave is less pronounced if compared with the impermeable barrier, but disturbances appear that catch up with the reflected wave. If the porosity increases, the free-surface evolution will become more regular as follows from Fig. 5c, where p = 0.25. The area of stochastic disturbances narrows here and there are no sharp rises and dips in the free surface. Fig. 5d shows the free-surface profiles formed when the solitary wave passes over the slotted barrier of Configuration 2. The dynamics of the free surface is changed here, though the porosity is the same as in Fig. 5c. It becomes more regular, and only small disturbances of the free surface are observed between the reflected and transmitted waves. It follows from Fig. 5 that the runup of the incident wave on the slotted barrier reduces when increasing its porosity. This leads to the loss of strength of the reflected wave, due to which the transmission wave grows indicating a deterioration in the protective properties of the structure. From this point of view, the barrier in Fig. 5c is the most unsuccessful, obviously because the total length of the solid elements decreases.

The conclusions following from the analysis of free-surface profiles are supported by evaluations of the hydraulic performance of slotted barriers in terms of wave reflection (R), transmission (T), and dissipation (D). The interaction of a solitary wave with a submerged obstacle can be quantified by the proportions either between the amplitudes or between the energies of the waves involved in the process. In this paper, energy wave coefficients are calculated:

$$k_t = \sqrt{E_t/E_i}, \qquad k_r = \sqrt{E_r/E_i}, \qquad k_d = \sqrt{E_d/E_i}.$$

Here,  $E_i$ ,  $E_t$ ,  $E_r$ ,  $E_d$  are the energy of incident, transmitted, and reflected waves, and the energy of dissipative processes respectively. To determine the wave energy, we applied the formulae of Li and Raichlen [52], in which the energy is calculated based on the wave amplitude and water depth. The energy scattered at the structure is defined according to the expression  $k_d^2 = 1 - k_r^2 - k_t^2$ . To verify the correctness of the calculation of RTD-coefficients in the present numerical experiment, their values were compared with the corresponding data from Lin [21] determined using the energy integral method. In the test, the propagation of the solitary wave of normalized amplitude  $A_i/h = 0.1$  over the submerged rectangle at

various combinations of its length and height is considered. The comparison of the obtained energy coefficients  $k_t$  and  $k_r$  with Lin's data is presented in Fig. 6. The normalized length of the structure a/h is plotted along the horizontal axis and two curves correspond to the different values of the structure height:d/h = 0.7 (red line) and d/h = 0.9 (blue line). The markers depict Lin's data. It can be seen that the comparison of the results shows the same trend for both  $k_r$  and  $k_t$  with an increase in the length of the structure in the range a/h = 0.1 to 3. The match for the coefficient  $k_t$  is much better than for  $k_r$ , which may be due to the difficulties in estimating the amplitude of a very small wave. In any case, these results confirm that the developed numerical algorithm adequately simulates the free-surface evolution when propagating a solitary wave over a submerged structure.

Further, the effect of porosity on the energy characteristics of wave decay over slotted barriers is assessed. Fig. 5 demonstrates a tendency to reduce the protective capacity of slotted structures compared to similar solid ones. Nevertheless, their use is advisable from the point of view of weakening environmental threats. Submerged barriers of various heights d/h and lengths a/h are considered here to identify their effective forms, although the main parameter whose influence is investigated is porosity p. In Fig. 7, the squared energy coeffi-

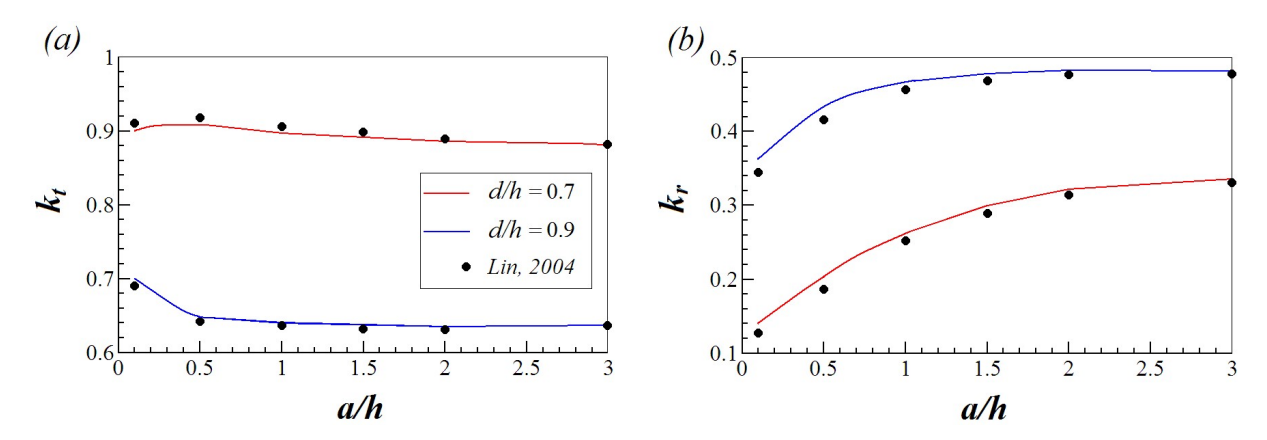


Fig. 6. Comparison of the wave energy coefficients  $k_t$  (a) and  $k_r$  (b) with the results from [21]

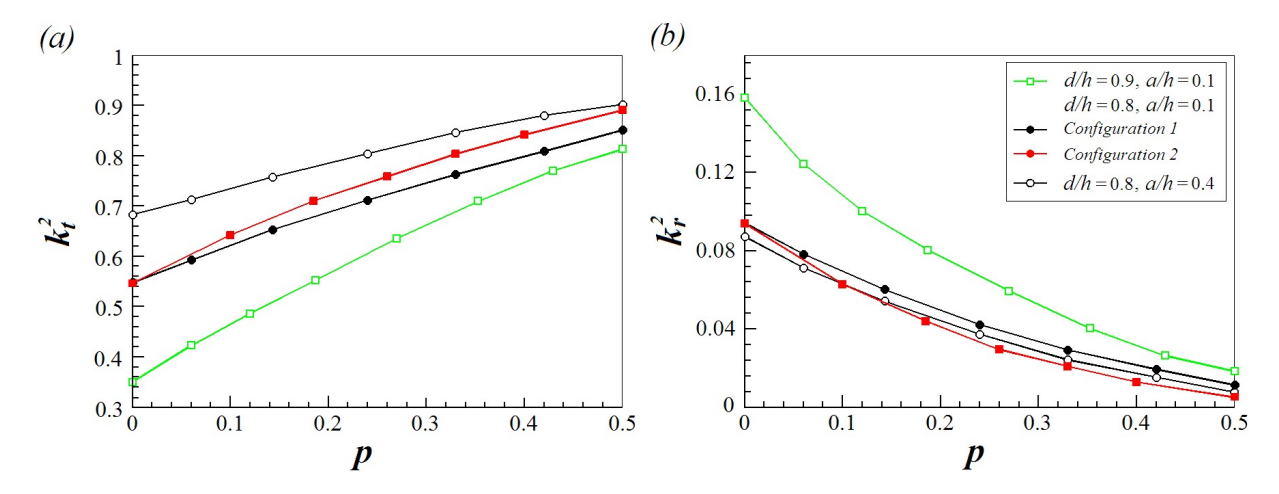


Fig. 7. Effect of porosity on the squared energy coefficients of solitary wave  $A_i/h = 0.2$  for slotted barriers of different heights and lengths: transmission (a) and reflection (b)

cients  $k_t^2$  (left) and reflection  $k_r^2$  (right) are depicted as functions of porosity calculated when interacting with the solitary wave of  $A_i/h = 0.2$  with slotted barriers of different geometrical parameters. Note that this representation provides direct information about the percentage of the energy associated with each process. The effect of the slotted barrier configuration on these coefficients is also analyzed here. As expected, the coefficient  $k_t^2$  grows with the increase of porosity in all the cases. However, the gradient of the curves in Fig. 7a differs significantly, which must be taken into account when choosing the most suitable breakwater design. It is known (e.g. [21,32]) that a high and short submerged barrier is the most effective in reducing the energy of incident waves. As can be seen in Fig. 7a at p=0, the energy of the transmitted wave behind the barrier of d/h = 0.8 is one and a half times higher than it when d/h = 0.9, with the same barrier length a/h = 0.1. However, the hydraulic performance of the high-slotted barrier sharply decreases with increasing its porosity. At p=0.5, the protective properties of the slotted barrier of height d/h = 0.9 drops by almost half compared to the same solid barrier. The amplification of the transmitted wave at d/h = 0.8 is not so catastrophic, especially with a large obstacle length, as the curve at a/h = 0.4 shows. Regarding the shape of the slotted barrier, Configuration 1 of those presented in Fig. 1 is preferable, obviously since the total length of the slots is lower here.

As follows from Fig. 7b, the energy of the reflected wave decreases to almost zero in the considered range of barrier porosity. Again, this process develops faster if the barrier is high. At d/h = 0.9 it was obtained that  $k_r^2 = 0.16$  at p = 0and  $k_r^2 = 0.02$  at p = 0.5. This means that the energy of the reflected wave decreases by approximately eight times. The functions  $k_r^2(p)$  at d/h = 0.8 demonstrate a similar trend, while they indicate a weak dependence of the reflection process on both the width and configuration of the structure. It follows

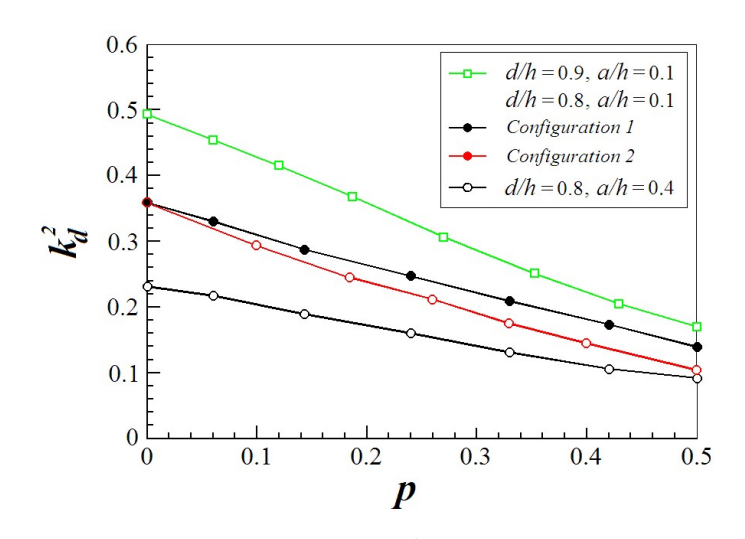


Fig. 8. Dependence of  $k_d^2$  on the porosity p

from these results that the influence of permeability on the reflection process is the main reason for the deterioration of the protective properties of the slotted wave breakwater.

The decrease in the energy dissipation coefficient with increasing barrier porosity is not so catastrophic, as evidenced by the results presented in Fig. 8. Note that dissipative wave energy losses occur due to both the formation of secondary disturbances on the free surface and the conversion of wave energy into the energy of the vortex field generated by the wave flow around the submerged structure. Since, disturbances on the water surface are attenuated with increasing porosity, as observed in Fig. 5, the influence of vorticity on dissipative processes should increase, which will be analyzed in the next section.

## 3.3. Development of a vortex field and formation of water exchange flows

The results of the previous section provide insight into the free-surface dynamics when a solitary wave interacts with a submerged slotted barrier. Wave propagation through the barrier is also accompanied by the processes developing in the water column, which must be taken into account when assessing the effectiveness of this obstacle as a breakwater. A traveling solitary wave generates an intense flow of liquid particles under the free surface. When this flow meets the barrier, it rebuilds according to the new configuration of the water area. The formation of a shear layer, flow separation and the development of a vortex field are successive manifestations of viscous effects caused by the wave. The vortex field helps dissipate wave energy but can compromise the integrity and stability of the structure due to large dynamic loads and bottom scouring, so it must be considered when designing protective structures.

Fig. 9 represents the vorticity and velocity fields in different transformation phases that develop when propagating the solitary wave of amplitude  $A_i/h = 0.2$  over the slotted barrier of Configuration 1 at d/h = 0.8, a/h = 0.1 and porosity p = 0.25. The scale of dimensionless vorticity is also depicted here. According to Madsen and Mei [9], the length  $L_s$  of a solitary wave is related to its amplitude by the ratio  $L_s/h \approx 10\sqrt{h/A_i}$ . It follows that  $L_s/h \approx 22$  in the case under consideration when  $A_i/h = 0.2$ . Thus, the formation of a shear layer near the submerged barrier begins when the wave crest is at a distance of about 11h. As the wave approaches, the negative pressure around the obstacle increases, as a result, the shear layer is separated on its walls converting into large-scale vortex structures.

One can see fully formed vortex pairs in the gaps between the barrier sections and a clockwise vortex at the top of the upper section when  $t\sqrt{g/h} \sim -2$  (Fig. 9a). These vortices grow as long as the local flow velocity near the obstacle increases, until  $t\sqrt{g/h} \sim 0$  (Fig. 9b). The following snapshots of the vorticity field correspond to the time instants when the wave crest has already passed over the top of the barrier. The development of fluid flows around the obstacle now depends on the dynamics of the vortex field. At the time instant shown in Fig. 9c, the part of counterclockwise vorticity (yellow) convects downstream, and new vortices are then generated at the lower edges of the barrier sections. When the clockwise vortices (blue) separate, they fall and block the path of the vortices located close to the barrier (Fig. 9d). Further, two counter-clockwise rotating vortices (yellow) merge to form a large vortex of the same direction of rotation near the upper barrier element. At that time, a large clockwise vortex structure (blue) develops near the foot of the barrier. These processes are finalized by the formation of a pair of oppositely rotating strong vortices on the leeward side of the barrier (Fig. 9e). Rotating, these vortices push the fluid through the gaps to the windward side. Moreover, the energy of the gap flows is sufficient in order to generate quite strong vortices there. The creation and evolution of vortex pairs on the windward side of the barrier are shown in snapshots Fig. 9f-h. It can also be noted that the scale of the vortices formed in the lower gap is significantly larger than those emerging from the upper gap. The vortex field on the leeward side of the barrier develops in such a way that most of the vorticity gets up towards the free surface, forming a large-scale clockwise vortex that follows the wave crest (Fig. 9h). Near the structure, the vortices diffuse slowly due to the complicated interactions with each other, as well as with the channel bottom and the barrier. It also follows from the analysis of the velocity fields presented in Fig. 9 that

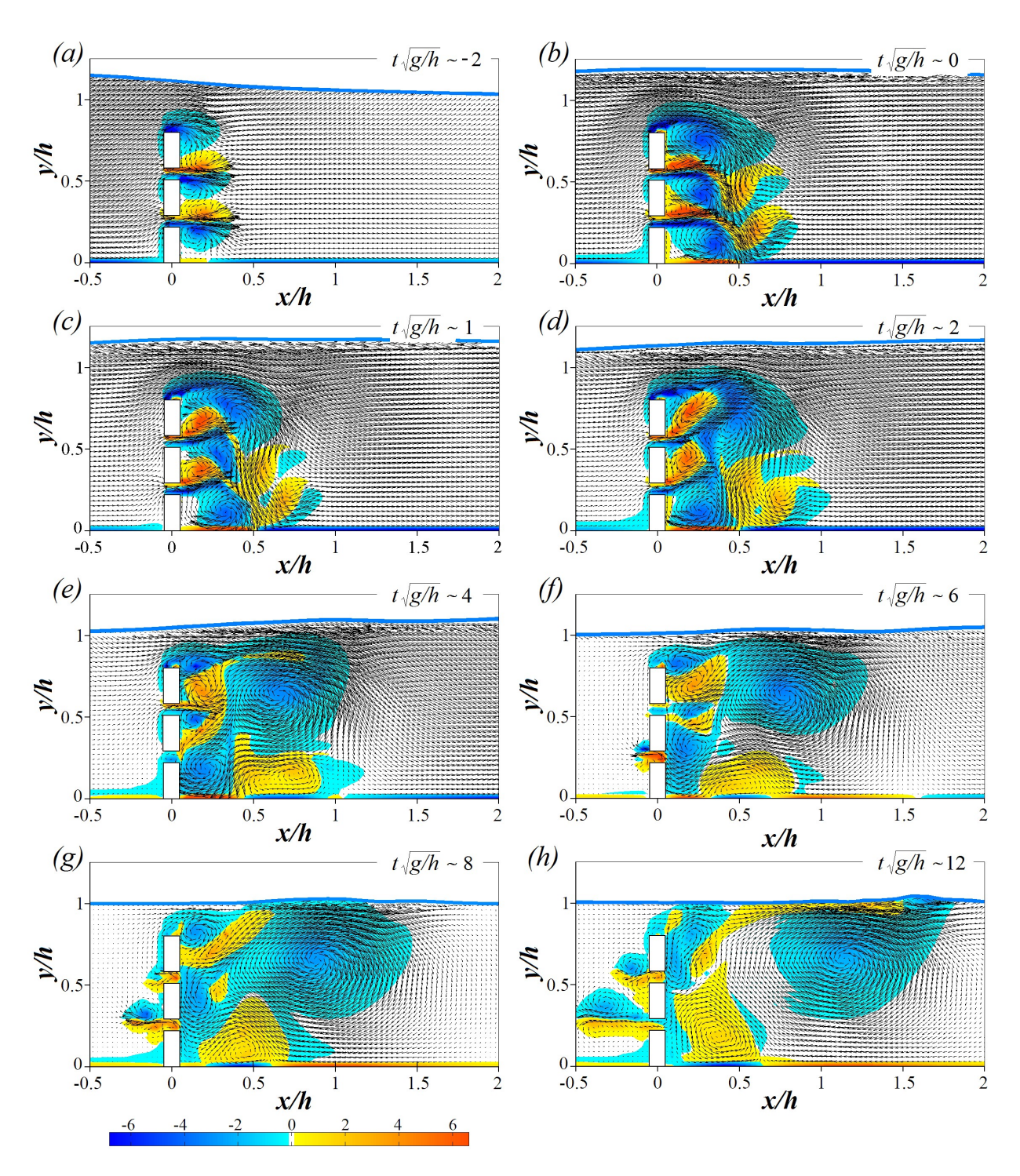


Fig. 9. Numerical visualization of the dynamics of vorticity and velocity fields generated by the solitary wave of  $A_i/h = 0.2$  near the slotted barrier of Configuration 1 at porosity  $p \approx 0.25$ 

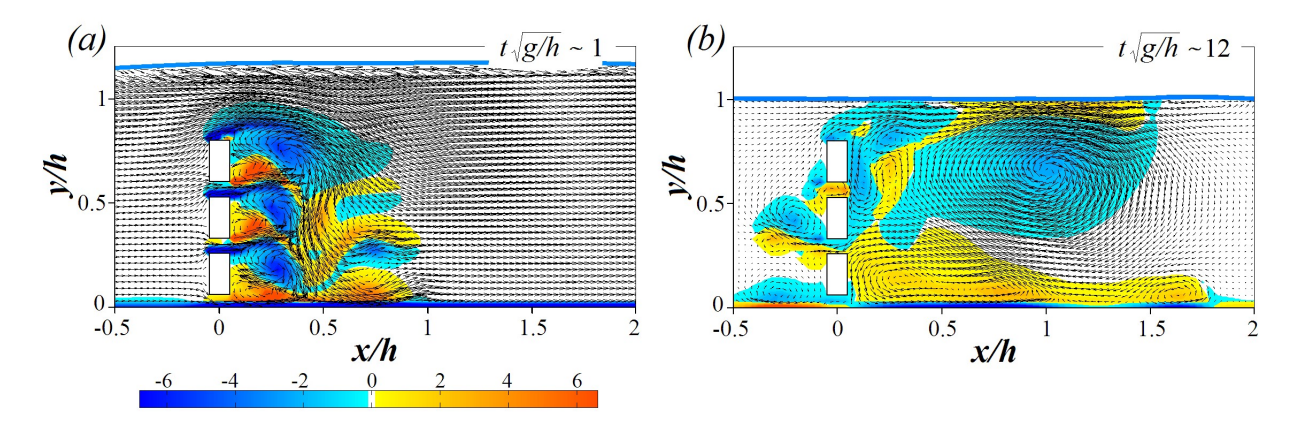


Fig. 10. Vorticity and velocity fields generated by the solitary wave of  $A_i/h = 0.2$  near the slotted barrier of Configuration 2 at porosity  $p \approx 0.25$  in various instants

traveling a solitary wave over a slotted barrier generates intense upward and downward flows on the leeward side, which causes the water mixing in this area.

In this numerical experiment, the influence of the slotted barrier configuration on the development of viscous processes was analyzed. We compared the vortex fields caused by the wave near the obstacles of the same porosity from those depicted in Fig. 1. The vorticity and velocity fields developed near the slotted barrier of *Configuration 2* at  $p \approx 0.25$  are depicted in Fig. 10.

The two presented snapshots correspond to the initial stage of wave-structure interaction and after a long time, when the vortex processes have self-organized. It is seen in Fig. 10a that the phenomena of flow separation occur at the lower and upper sides of each barrier element, which results in the formation of three pairs of counter-rotating vortices on the leeward side of the obstacle. Further, the vortices interact with each other, with free surface and with solid boundaries that leads to the stage of vortex field presented in Fig. 10b. This flow pattern is similar to that observed in Fig. 9h. It is characterized by the generation of reverse flows in the gaps between the barrier sections, as well as by the development of vortex pairs on the windward side and large-scale vortices on the leeward side of the barrier. Among the distinctions between the snapshots depicted in Fig. 10b and Fig. 9h one can notice a weak reverse flow in the gap between the lover element of the barrier and the channel bottom. Because of this, the intensity of the reverse flows in the other two gaps decreases, as a result, the vortices to have formed on the windward side are weakened compared to the corresponding time instant in Fig. 9. On the leeward side of the barrier, a large-scale clockwise vortex (blue) gets up to the free surface as in the previous case. The counterclockwise vorticity (yellow) in Fig. 10b extends along the channel bottom in contrast to the distinct vortex observed in Fig. 9h. To summarize, it can be concluded that the evolution of the vortex field weakly depends on the arrangement of the barrier elements in the same porosity.

More visual differences in the development of the vortex field will be observed if the distance between the barrier sections is increased. Fig. 11 illustrates the vortex fields obtained near the slotted barriers of both considered configurations at  $p \approx 0.5$ . It can be seen that they differ little from each other. At the same time, their distinction from the corresponding

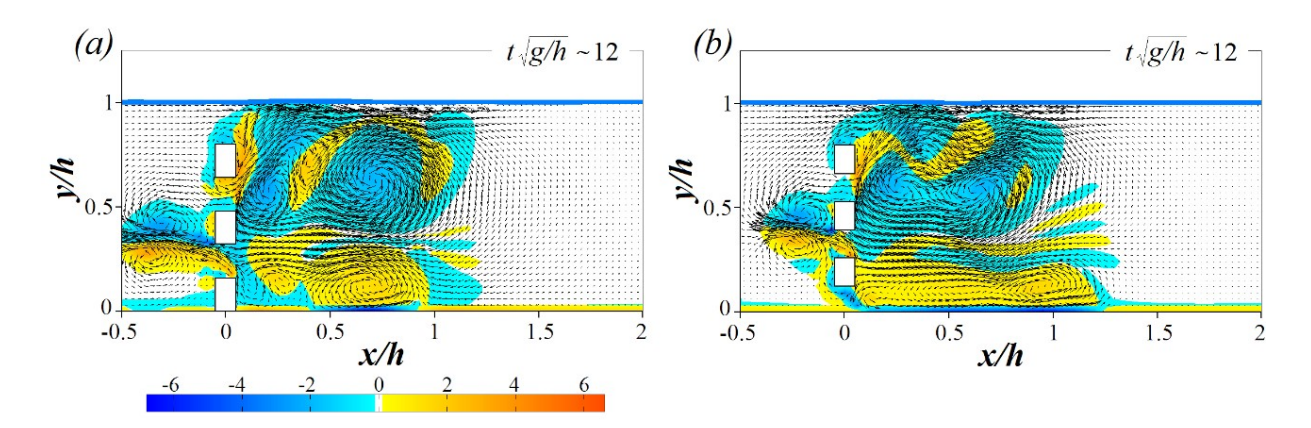


Fig. 11. Vorticity and velocity fields generated by the solitary wave of  $A_i/h = 0.2$  near the slotted barrier of Configuration 1 (left) and Configuration 2 (right) at  $p \approx 0.5$ 

snapshots presented in Fig. 9 and Fig. 10 is obvious. In particular, the reverse flow in both Configuration 1 and Configuration 2 develops only in the gap between the lower section and the one adjacent to it, due to which the vortex pair formed here has a much larger scale and strength than with lower barrier porosity. The interaction of vortices on the leeward side of the barrier occurs in such a way that it does not lead to a dominant vortex here, as in the previous cases. Instead, several pairs of counter-rotating vortices of approximately equal size and strength are formed. These vortices interact weakly with the free surface and remain close to the structure, apparently, until they gradually diffuse.

Careful examination of the velocity fields in Figs. 9-11 reveals the development of water flows around the structure. The interaction of vortices on the leeward side causes the flows directed toward the bottom and vice versa, which replace one another. This supports the exchange between bottom and surface waters, thereby sustaining the health of the coastal ecology by creating an upwelling effect. Another important requirement for improving the environment is to ensure water exchange between the open sea and the coastal zone when the water area is blocked by the submerged barrier. Making slots in the barrier is aimed at solving this problem, although the protective properties of the structure deteriorate. The development of reverse flows is seen in Figs. 9-11. To quantitatively assess this process, let us analyze the longitudinal velocity profiles in the cross-section  $\bar{x}=0$ . Fig. 12 illustrates the distributions of the normalized longitudinal velocity  $\bar{u} = u/\sqrt{gh}$  along the central line of the slotted barrier of Configuration 1 at porosity  $p \approx 0.25$ . The curves in Fig. 12a correspond to the time  $\bar{t} < 0$ , when the wave crest either approaches the obstacle or is above it. The velocity is seen to increase over the obstacle and in the gaps, and reaches its maximum value at  $\bar{t} \approx 0$ . After the crest of the wave passes the obstacle, water flows are determined by the dynamics of the vortex field. It is clear in Fig. 12b, corresponding to this period, that  $\bar{u}$ decreases in the slots. The highest reverse flow velocity occurs in the lower gap at  $\bar{t} \approx 8$  and then it decreases, which indicates that the flow is attenuated here. In the upper gap, on the contrary, the small initial velocity  $\bar{u}$  attenuates much more slowly.

Based on the longitudinal velocity, the water discharge Q in the cross-section  $\bar{x}=0$  was calculated for slotted barriers of various porosities and configurations. Counterflows are analyzed separately, assuming that Q>0 describes the flow of water in the direction of

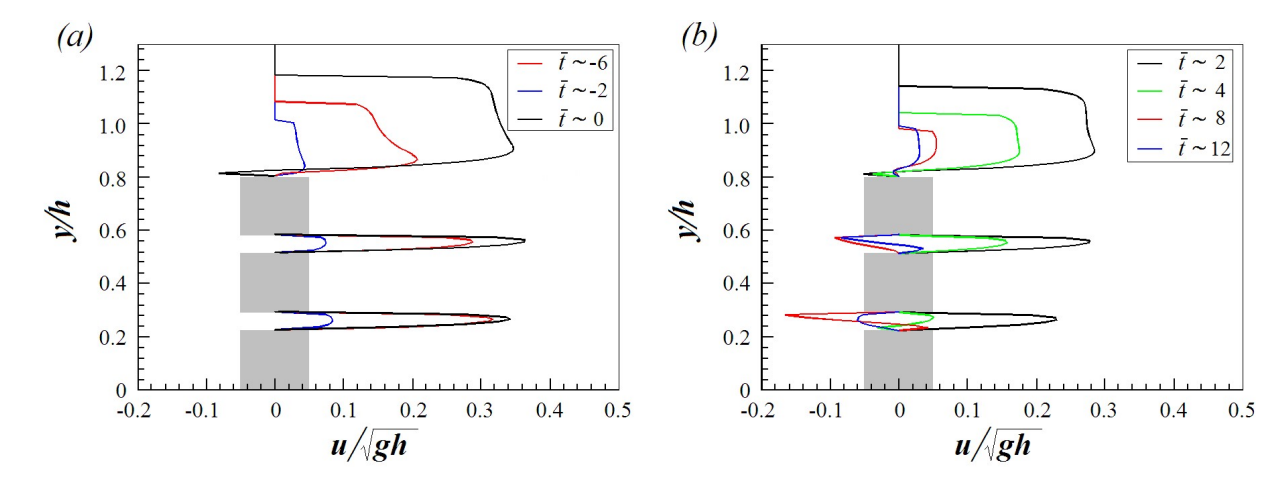


Fig. 12. Horizontal velocity profiles induced by the solitary wave of amplitude  $A_i/h = 0.2$  along the central line of the slotted barrier at different time instants

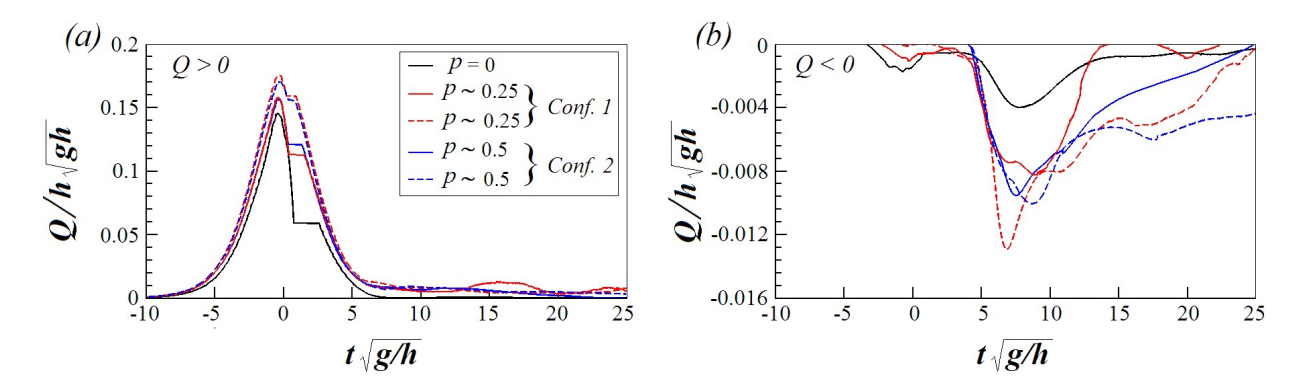


Fig. 13. Time dependences of the intensities of the water exchange flows in the cross-section x = 0 generated when propagating the solitary wave of amplitude  $A_i/h = 0.2$  over slotted barriers of various porosity and configuration

wave propagation and Q < 0 corresponds to the opposite direction. Fig. 13 illustrates the dependencies of the normalized discharge of the direct and reverse flows on time. The black lines in these pictures describe the water discharge over the impermeable barrier of height d/h = 0.8. The red and blue lines correspond to the slotted barriers of the same height in Configuration 1 and Configuration 2 respectively; solid and dashed lines are calculated at various porosities,  $p \approx 0.25$  and  $p \approx 0.5$ . It follows from Fig. 13a that a solitary wave propagating over the submerged barrier forms the water flow directed to the coastline. The flow rate achieves its maximum when the wave crest is above the obstacle and drops to almost zero at  $\bar{t} > 5$ . This means that the wave is no longer the dominant factor in the region disposed near the obstacle. Fig. 13a points out that the forward flow rate weakly depends on the porosity of the barrier and is almost independent of its configuration at the same barrier height. This happens because most of the water passes between the top of the barrier and the free surface.

As mentioned above, the reverse flow is formed under the influence of the vortex field. It can be seen in Fig. 13b that its rate is an order of magnitude less than that of the forward flow. However, it is remarkable that the use of a slotted barrier increases the rate of reverse

flow several times when compared with an impermeable barrier. The reverse flow is the most intense in the period  $5 < \bar{t} < 10$  and it is unlikely to see a reliable trend in its development since this flow is controlled by the stochastic interaction of vortices. We calculated that the total amount of water passing through the section  $\bar{x} = 0$  in the reverse direction during the entire numerical experiment increased in proportion to the growing porosity and did not depend on the barrier configuration.

## 4. CONCLUSIONS

In this study, the interaction of a solitary wave with a submerged slotted barrier was numerically investigated with respect to the effectiveness of such a structure against waves and care for the environment. The numerical procedure is based on a combination of the boundary integral method, which describes deformations of the free surface, and the hybrid vortex scheme used to simulate the viscous flow under the free surface. The procedure was validated by our own experimental results as well as by numerical and experimental data known from other studies available in the literature.

In the calculations, the porosity and configuration of the slotted barrier were varied to find an optimal solution that takes into account both the hydraulic performance of the barrier as a breakwater and its capability to generate water exchange flows between the open sea and the coastal zone. The results obtained are assumed to allow reducing the efforts and financial costs for the construction of this kind of protective structure.

The barrier porosity was changed from 0 to 0.5, and two configurations of the structure were considered when its lower element either lies on the bottom or there is a gap between this element and the seabed. A solitary wave of non-dimensional amplitude  $A_i/h = 0.2$  was examined for the entire numerical experiment. Analysis of the free-surface evolution, as well as energy transmission and reflection coefficients, revealed that the protective properties of the structure deteriorate with increasing barrier porosity. The permeability has been found to have a greater effect on high and narrow barriers than on lower and wider ones. In addition, Configuration 1 is preferable due to its hydraulic performance.

A study of viscous effects created by the solitary wave around a slotted barrier demonstrated the development of large-scale counter-rotating vortices on the leeward side of the obstacle. Their interactions cause the generation of reverse flows in the gaps between the barrier elements, which is accompanied by the formation of vortex pairs on the windward side. It has been established that the rate of the water flows directed opposite to the wave propagation depends more on the distance between the solid elements than on their layout. When testing various slotted barriers, an increase in the rate of reverse flow several times was revealed compared to the same impenetrable barrier.

The data obtained in this numerical experiment indicate that a slotted barrier of porosity 0.2 to 0.3 will be the most successful among structures of this type for shore protection and for sustaining the health of the coastal ecology.

#### REFERENCES

[1] D. L. Kriebel, "Vertical wave barriers: wave transmission and wave forces," in *Coastal Engineering Proceedings*, vol. 1(23). Orlando, FL: ICCE, 1992, pp. 1313–1326. DOI: https://doi.org/10.1061/9780872629332.099

- [2] C. Lin, T.-C. Ho, S.-C. Chang, S.-C. Hsieh, and K.-A. Chang, "Vortex shedding induced by a solitary wave propagating over a submerged vertical plate," *International Journal of Heat and Fluid Flow*, vol. 26, no. 6, pp. 894–904, 2005. DOI: https://doi.org/10.1016/j.ijheatfluidflow.2005.10.009
- [3] I. M. Gorban, A. C. Korolova, and O. G. Lebid, "Interaction of surface solitary wave with submerged and semi-submerged breakwaters," *Precarpathian Bulletin of the Shevchenko Scientific Society "Number"*, no. 17(64), pp. 118–132, 2022. DOI: https://doi.org/10.31471/2304-7399-2022-17(64)-118-132
- [4] M. Isaacson, S. Premasiri, and G. Yang, "Wave interactions with vertical slotted barrier," *Journal of Waterway, Port, Coastal, and Ocean Engineering*, vol. 124, no. 3, pp. 118–126, 1998. DOI: https://doi.org/10.1061/(asce)0733-950x(1998)124:3(118)
- [5] M. Isaacson, J. Baldwin, S. Premasiri, and G. Yang, "Wave interactions with double slotted barriers," Applied Ocean Research, vol. 21, no. 2, pp. 81–91, 1999. DOI: https://doi.org/10.1016/s0141-1187(98)00039-x
- [6] O. S. Rageh and A. S. Koraim, "Hydraulic performance of vertical walls with horizontal slots used as breakwater," Coastal Engineering, vol. 57, no. 8, pp. 745–756, 2010. DOI: https://doi.org/10.1016/j.coastaleng.2010.03.005
- [7] Z. Huang, Y. Li, and Y. Liu, "Hydraulic performance and wave loadings of perforated/slotted coastal structures: A review," *Ocean Engineering*, vol. 38, no. 10, pp. 1031–1053, 2011. DOI: https://doi.org/10.1016/j.oceaneng.2011.03.002
- [8] C. E. Synolakis, "The runup of solitary waves," Journal of Fluid Mechanics, vol. 185, pp. 523–545, 1987. DOI: https://doi.org/10.1017/s002211208700329x
- [9] O. S. Madsen and C. C. Mei, "The transformation of a solitary wave over an uneven bottom," *Journal of Fluid Mechanics*, vol. 39, no. 4, pp. 781–791, 1969. DOI: https://doi.org/10.1017/s0022112069002461
- [10] F. J. Seabra-Santos, D. P. Renouard, and A. M. Temperville, "Numerical and experimental study of the transformation of a solitary wave over a shelf or isolated obstacle," *Journal of Fluid Mechanics*, vol. 176, no. 1, p. 117, 1987. DOI: https://doi.org/10.1017/s0022112087000594
- [11] M. A. Losada, C. Vidal, and R. Medina, "Experimental study of the evolution of a solitary wave at an abrupt junction," *Journal of Geophysical Research: Oceans*, vol. 94, no. C10, pp. 14557–14566, 1989. DOI: https://doi.org/10.1029/jc094ic10p14557
- [12] P. A. Madsen, R. Murray, and O. R. Sørensen, "A new form of the Boussinesq equations with improved linear dispersion characteristics," *Coastal Engineering*, vol. 15, no. 4, pp. 371–388, 1991. DOI: https://doi.org/10.1016/0378-3839(91)90017-b
- [13] S. Beji and J. A. Battjes, "Numerical simulation of nonlinear wave propagation over a bar," Coastal Engineering, vol. 23, no. 1-2, pp. 1–16, 1994. DOI: https://doi.org/10.1016/0378-3839(94)90012-4

- [14] Q. Chen, J. T. Kirby, R. A. Dalrymple, A. B. Kennedy, and A. Chawla, "Boussinesq modeling of wave transformation, breaking, and runup. II: 2D," *Journal of Waterway*, *Port, Coastal, and Ocean Engineering*, vol. 126, no. 1, pp. 48–56, 2000. DOI: https://doi.org/10.1061/(asce)0733-950x(2000)126:1(48)
- [15] J. Kim, G. K. Pedersen, F. Løvholt, and R. J. LeVeque, "A Boussinesq type extension of the GeoClaw model a study of wave breaking phenomena applying dispersive long wave models," *Coastal Engineering*, vol. 122, pp. 75–86, 2017. DOI: https://doi.org/10.1016/j.coastaleng.2017.01.005
- [16] M. J. Cooker, D. H. Peregrine, C. Vidal, and J. W. Dold, "The interaction between a solitary wave and a submerged semicircular cylinder," *Journal of Fluid Mechanics*, vol. 215, no. 1, pp. 1–22, 1990. DOI: https://doi.org/10.1017/s002211209000252x
- [17] S. T. Grilli, M. A. Losada, and F. Martin, "Characteristics of solitary wave breaking induced by breakwaters," *Journal of Waterway, Port, Coastal, and Ocean Engineering*, vol. 120, no. 1, pp. 74–92, 1994. DOI: https://doi.org/10.1061/(asce)0733-950x(1994)120:1(74)
- [18] Y. Cheng, G. Li, C. Ji, and G. Zhai, "Solitary wave slamming on an oscillating wave surge converter over varying topography in the presence of collinear currents," *Physics of Fluids*, vol. 32, no. 4, p. 047102, 2020. DOI: https://doi.org/10.1063/5.0001402
- [19] C.-J. Tang and J.-H. Chang, "Flow separation during solitary wave passing over submerged obstacle," *Journal of Hydraulic Engineering*, vol. 124, no. 7, pp. 742–749, 1998. DOI: https://doi.org/10.1061/(asce)0733-9429(1998)124:7(742)
- [20] P. Lin and P. L.-F. Liu, "A numerical study of breaking waves in the surf zone," *Journal of Fluid Mechanics*, vol. 359, pp. 239–264, 1998. DOI: https://doi.org/10.1017/s002211209700846x
- [21] P. Lin, "A numerical study of solitary wave interaction with rectangular obstacles," Coastal Engineering, vol. 51, no. 1, pp. 35–51, 2004. DOI: https://doi.org/10.1016/j.coastaleng.2003.11.005
- [22] K.-A. Chang, T.-J. Hsu, and P. L.-F. Liu, "Vortex generation and evolution in water waves propagating over a submerged rectangular obstacle," *Coastal Engineering*, vol. 44, no. 1, pp. 13–36, 2001. DOI: https://doi.org/10.1016/s0378-3839(01)00019-9
- [23] C.-J. Huang and C.-M. Dong, "On the interaction of a solitary wave and a submerged dike," Coastal Engineering, vol. 43, no. 3-4, pp. 265–286, 2001. DOI: https://doi.org/10.1016/s0378-3839(01)00017-5
- [24] Y.-T. Wu, S.-C. Hsiao, Z.-C. Huang, and K.-S. Hwang, "Propagation of solitary waves over a bottom-mounted barrier," *Coastal Engineering*, vol. 62, pp. 31–47, 2012. DOI: https://doi.org/10.1016/j.coastaleng.2012.01.002
- [25] J. J. Monaghan, "Simulating free surface flows with SPH," Journal of Computational Physics, vol. 110, no. 2, pp. 399–406, 1994. DOI: https://doi.org/10.1006/jcph.1994.1034

- [26] S. Koshizuka, A. Nobe, and Y. Oka, "Numerical analysis of breaking waves using the moving particle semi-implicit method," *International Journal for Numerical Methods in Fluids*, vol. 26, no. 7, pp. 751–769, 1998. DOI: https://doi.org/10.1002/(sici)1097-0363(19980415)26:7\(\frac{7}{51}::aid-fld671\)\(\frac{3}{3}.0.co;2-c\)
- [27] Y. Ren, M. Luo, and P. Lin, "Consistent particle method simulation of solitary wave interaction with a submerged breakwater," *Water*, vol. 11, no. 2, p. 261, 2019. DOI: https://doi.org/10.3390/w11020261
- [28] X. Han and S. Dong, "Interaction of solitary wave with submerged breakwater by smoothed particle hydrodynamics," *Ocean Engineering*, vol. 216, p. 108108, 2020. DOI: https://doi.org/10.1016/j.oceaneng.2020.108108
- [29] Y. Huang and C. Zhu, "Numerical analysis of tsunami–structure interaction using a modified MPS method," *Natural Hazards*, vol. 75, no. 3, pp. 2847–2862, 2014. DOI: https://doi.org/10.1007/s11069-014-1464-1
- [30] P. Koumoutsakos, A. Leonard, and F. Pépin, "Boundary conditions for viscous vortex methods," *Journal of Computational Physics*, vol. 113, no. 1, pp. 52–61, 1994. DOI: https://doi.org/10.1006/jcph.1994.1117
- [31] M.-Y. Lin and L.-H. Huang, "Vortex shedding from a submerged rectangular obstacle attacked by a solitary wave," *Journal of Fluid Mechanics*, vol. 651, pp. 503–518, 2010. DOI: https://doi.org/10.1017/s0022112010000145
- [32] I. M. Gorban and A. S. Korolyova, "Numerical simulation of the interaction of a soliton wave with immersed obstacles," *Visnyk of Zaporizhzhya National University Physical and Mathematical Sciences*, no. 1, pp. 22–32, 2021. DOI: https://doi.org/10.26661/2413-6549-2021-1-03
- [33] P. L.-F. Liu and K. Al-Banaa, "Solitary wave runup and force on a vertical barrier," *Journal of Fluid Mechanics*, vol. 505, pp. 225–233, 2004. DOI: https://doi.org/10.1017/s0022112004008547
- [34] S. Shao, "SPH simulation of solitary wave interaction with a curtain-type breakwater," *Journal of Hydraulic Research*, vol. 43, no. 4, pp. 366–375, 2005. DOI: https://doi.org/10.1080/00221680509500132
- [35] M. J. Ketabdari, N. Kamani, and M. H. Moghaddam, "WCSPH simulation of solitary wave interaction with a curtain-type breakwater," in AIP Conference Proceedings, vol. 1648. AIP Publishing LLC, 2015, p. 770006. DOI: https://doi.org/10.1063/1.4912976
- [36] Y.-T. Wu, S.-C. Hsiao, K.-S. Hwang, T.-C. Lin, and A. Torres-Freyermuth, "Numerical study of solitary wave interaction with a slotted barrier," in *International Ocean and Polar Engineering Conference*. Maui, HI: International Society of Offshore and Polar Engineers, 2011, pp. ISOPE–I–11–072.

- [37] Y.-T. Wu and S.-C. Hsiao, "Propagation of solitary waves over a submerged slotted barrier," *Journal of Marine Science and Engineering*, vol. 8, no. 6, p. 419, 2020. DOI: https://doi.org/10.3390/jmse8060419
- [38] V. O. Gorban and I. M. Gorban, "Vortical flow structure near a square prism: numerical model and algorithms of control," *Applied Hydromechanics*, vol. 7(79), no. 2, pp. 8–26, 2005.
- [39] I. M. Gorban, A numerical study of solitary wave interactions with a bottom step. Cham, Germany: Springer International Publishing, 2015, pp. 369–387. DOI: https://doi.org/10.1007/978-3-319-19075-4\_22
- [40] J. G. Telste, "Potential flow about two counter-rotating vortices approaching a free surface," *Journal of Fluid Mechanics*, vol. 201, no. 1, p. 259, 1989. DOI: https://doi.org/10.1017/s0022112089000935
- [41] G. R. Baker, D. I. Meiron, and S. A. Orszag, "Generalized vortex methods for free-surface flow problems," *Journal of Fluid Mechanics*, vol. 123, pp. 477–501, 1982. DOI: https://doi.org/10.1017/s0022112082003164
- [42] H. Lamb, Hydrodynamics. Cambridge, UK: Cambridge University Press, 1932.
- [43] G.-H. Cottet and Р. D. Koumoutsakos, Vortex methods: theory and practice. Cambridge, UK: Cambridge University Press, 2000. DOI: https://doi.org/10.1017/cbo9780511526442
- [44] I. M. Gorban and O. V. Khomenko, Flow control near a square prism with the help of frontal flat plates. Cham, Germany: Springer International Publishing, 2016, pp. 327–350. DOI: https://doi.org/10.1007/978-3-319-40673-2\_17
- [45] I. M. Gorban and O. G. Lebid, Numerical modeling of the wing aerodynamics at angle-of-attack at low Reynolds numbers. Cham, Germany: Springer International Publishing, 2018, pp. 159–179. DOI: https://doi.org/10.1007/978-3-319-96755-4\_10
- [46] D. Clamond and D. Dutykh, "Fast accurate computation of the fully nonlinear solitary surface gravity waves," *Computers & Fluids*, vol. 84, pp. 35–38, 2013. DOI: https://doi.org/10.1016/j.compfluid.2013.05.010
- [47] A. S. Kotelnikova, V. I. Nikishov, and S. M. Srebnyuk, "On the interaction of surface solitary waves and underwater obstacles," Reports of the National Academy of Sciences of Ukraine, no. 7, pp. 54–59, 2012.
- [48] J. G. B. Byatt-Smith, "An integral equation for unsteady surface waves and a comment on the Boussinesq equation," *Journal of Fluid Mechanics*, vol. 49, no. 4, pp. 625–633, 1971. DOI: https://doi.org/10.1017/s0022112071002295
- [49] R. K.-C. Chan and R. L. Street, "A computer study of finite-amplitude water waves," *Journal of Computational Physics*, vol. 6, no. 1, pp. 68–94, 1970. DOI: https://doi.org/10.1016/0021-9991(70)90005-7

- "Experiments on collisions waves," [50] T. Maxworthy, between solitary Jourof Fluid Mechanics, vol. 76, 1, 177-186, 1976. DOI: no. pp. https://doi.org/10.1017/s0022112076003194
- [51] D. Lo and D. Young, "Arbitrary Lagrangian-Eulerian finite element analysis of free surface flow using a velocity-vorticity formulation," *Journal of Computational Physics*, vol. 195, no. 1, pp. 175–201, 2004. DOI: https://doi.org/10.1016/j.jcp.2003.09.019
- [52] Y. Li and F. Raichlen, "Energy balance model for breaking solitary wave runup," Journal of Waterway, Port, Coastal, and Ocean Engineering, vol. 129, no. 2, pp. 47–59, 2003. DOI: https://doi.org/10.1061/(asce)0733-950x(2003)129:2(47)

#### ЛІТЕРАТУРА

- [1] Kriebel D. L. Vertical wave barriers: wave transmission and wave forces // Coastal Engineering Proceedings. Orlando, FL: ICCE. 1992. Vol. 1(23). P. 1313—1326.
- [2] Vortex shedding induced by a solitary wave propagating over a submerged vertical plate / Lin C., Ho T.-C., Chang S.-C., Hsieh S.-C., and Chang K.-A. // International Journal of Heat and Fluid Flow. 2005. Vol. 26, no. 6. P. 894–904.
- [3] Горбань І. М., Корольова А. С., Лебідь О. Г. Взаємодія поверхневої поодинокої хвилі із зануреним та напівзануреним хвилегасниками // Прикарпатський вісник наукового товариства імені Шевченка «Число». 2022. № 17(64). С. 118—132.
- [4] Isaacson M., Premasiri S., Yang G. Wave interactions with vertical slotted barrier // Journal of Waterway, Port, Coastal, and Ocean Engineering. 1998. Vol. 124, no. 3. P. 118–126.
- [5] Wave interactions with double slotted barriers / Isaacson M., Baldwin J., Premasiri S., and Yang G. // Applied Ocean Research. 1999. Vol. 21, no. 2. P. 81–91.
- [6] Rageh O. S., Koraim A. S. Hydraulic performance of vertical walls with horizontal slots used as breakwater // Coastal Engineering. 2010. Vol. 57, no. 8. P. 745–756.
- [7] Huang Z., Li Y., Liu Y. Hydraulic performance and wave loadings of perforated/slotted coastal structures: A review // Ocean Engineering. 2011. Vol. 38, no. 10. P. 1031–1053.
- [8] Synolakis C. E. The runup of solitary waves // Journal of Fluid Mechanics. 1987. Vol. 185. P. 523–545.
- [9] Madsen O. S., Mei C. C. The transformation of a solitary wave over an uneven bottom // Journal of Fluid Mechanics. 1969. Vol. 39, no. 4. P. 781–791.
- [10] Seabra-Santos F. J., Renouard D. P., Temperville A. M. Numerical and experimental study of the transformation of a solitary wave over a shelf or isolated obstacle // Journal of Fluid Mechanics. 1987. Vol. 176, no. 1. P. 117.

- [11] Losada M. A., Vidal C., Medina R. Experimental study of the evolution of a solitary wave at an abrupt junction // Journal of Geophysical Research: Oceans. 1989. Vol. 94, no. C10. P. 14557–14566.
- [12] Madsen P. A., Murray R., Sørensen O. R. A new form of the Boussinesq equations with improved linear dispersion characteristics // Coastal Engineering. 1991. Vol. 15, no. 4. P. 371–388.
- [13] Beji S., Battjes J. A. Numerical simulation of nonlinear wave propagation over a bar // Coastal Engineering. 1994. Vol. 23, no. 1-2. P. 1–16.
- [14] Boussinesq modeling of wave transformation, breaking, and runup. II: 2D / Chen Q., Kirby J. T., Dalrymple R. A., Kennedy A. B., and Chawla A. // Journal of Waterway, Port, Coastal, and Ocean Engineering. 2000. Vol. 126, no. 1. P. 48–56.
- [15] A Boussinesq type extension of the GeoClaw model a study of wave breaking phenomena applying dispersive long wave models / Kim J., Pedersen G. K., Løvholt F., and LeVeque R. J. // Coastal Engineering. 2017. Vol. 122. P. 75–86.
- [16] The interaction between a solitary wave and a submerged semicircular cylinder / Cooker M. J., Peregrine D. H., Vidal C., and Dold J. W. // Journal of Fluid Mechanics. 1990. Vol. 215, no. 1. P. 1–22.
- [17] Grilli S. T., Losada M. A., Martin F. Characteristics of solitary wave breaking induced by breakwaters // Journal of Waterway, Port, Coastal, and Ocean Engineering. 1994. Vol. 120, no. 1. P. 74–92.
- [18] Solitary wave slamming on an oscillating wave surge converter over varying topography in the presence of collinear currents / Cheng Y., Li G., Ji C., and Zhai G. // Physics of Fluids. 2020. Vol. 32, no. 4. P. 047102.
- [19] Tang C.-J., Chang J.-H. Flow separation during solitary wave passing over submerged obstacle // Journal of Hydraulic Engineering. 1998. Vol. 124, no. 7. P. 742–749.
- [20] Lin P., Liu P. L.-F. A numerical study of breaking waves in the surf zone // Journal of Fluid Mechanics. 1998. Vol. 359. P. 239–264.
- [21] Lin P. A numerical study of solitary wave interaction with rectangular obstacles // Coastal Engineering. 2004. Vol. 51, no. 1. P. 35–51.
- [22] Chang K.-A., Hsu T.-J., Liu P. L.-F. Vortex generation and evolution in water waves propagating over a submerged rectangular obstacle // Coastal Engineering. 2001. Vol. 44, no. 1. P. 13–36.
- [23] Huang C.-J., Dong C.-M. On the interaction of a solitary wave and a submerged dike // Coastal Engineering. 2001. Vol. 43, no. 3-4. P. 265–286.
- [24] Propagation of solitary waves over a bottom-mounted barrier / Wu Y.-T., Hsiao S.-C., Huang Z.-C., and Hwang K.-S. // Coastal Engineering. 2012. Vol. 62. P. 31–47.

- [25] Monaghan J. J. Simulating free surface flows with SPH // Journal of Computational Physics. 1994. Vol. 110, no. 2. P. 399–406.
- [26] Koshizuka S., Nobe A., Oka Y. Numerical analysis of breaking waves using the moving particle semi-implicit method // International Journal for Numerical Methods in Fluids. 1998. Vol. 26, no. 7. P. 751–769.
- [27] Ren Y., Luo M., Lin P. Consistent particle method simulation of solitary wave interaction with a submerged breakwater // Water. 2019. Vol. 11, no. 2. P. 261.
- [28] Han X., Dong S. Interaction of solitary wave with submerged breakwater by smoothed particle hydrodynamics // Ocean Engineering. 2020. Vol. 216. P. 108108.
- [29] Huang Y., Zhu C. Numerical analysis of tsunami–structure interaction using a modified MPS method // Natural Hazards.—2014.—Vol. 75, no. 3.—P. 2847–2862.
- [30] Koumoutsakos P., Leonard A., Pépin F. Boundary conditions for viscous vortex methods // Journal of Computational Physics. 1994. Vol. 113, no. 1. P. 52–61.
- [31] Lin M.-Y., Huang L.-H. Vortex shedding from a submerged rectangular obstacle attacked by a solitary wave // Journal of Fluid Mechanics. 2010. Vol. 651. P. 503—518.
- [32] Горбань І. М., Корольова А. С. Чисельне моделювання взаємодії солітонної хвилі із зануреними перешкодами // Computer Science and Applied Mathematics. 2021. N = 1. С. 22–32.
- [33] Liu P. L.-F., Al-Banaa K. Solitary wave runup and force on a vertical barrier // Journal of Fluid Mechanics. 2004. Vol. 505. P. 225–233.
- [34] Shao S. SPH simulation of solitary wave interaction with a curtain-type breakwater // Journal of Hydraulic Research. 2005. Vol. 43, no. 4. P. 366–375.
- [35] Ketabdari M. J., Kamani N., Moghaddam M. H. WCSPH simulation of solitary wave interaction with a curtain-type breakwater // AIP Conference Proceedings. AIP Publishing LLC. 2015. Vol. 1648. P. 770006.
- [36] Numerical study of solitary wave interaction with a slotted barrier / Wu Y.-T., Hsiao S.-C., Hwang K.-S., Lin T.-C., and Torres-Freyermuth A. // International Ocean and Polar Engineering Conference. Maui, HI: International Society of Offshore and Polar Engineers. 2011. P. ISOPE-I-11-072.
- [37] Wu Y.-T., Hsiao S.-C. Propagation of solitary waves over a submerged slotted barrier // Journal of Marine Science and Engineering. 2020. Vol. 8, no. 6. P. 419.
- [38] Горбань В. О., Горбань І. М. Вихрова структура потоку при обтіканні квадратної призми: числова модель та алгоритми управління // Прикладна гідромеханіка. 2005. Т. 7(79), № 2. С. 8–26.

- [39] Gorban I. M. A numerical study of solitary wave interactions with a bottom step // Continuous and Distributed Systems. II. Studies in Systems, Decision and Control. Cham, Germany: Springer International Publishing, 2015. P. 369–387.
- [40] Telste J. G. Potential flow about two counter-rotating vortices approaching a free surface // Journal of Fluid Mechanics. 1989. Vol. 201, no. 1. P. 259.
- [41] Baker G. R., Meiron D. I., Orszag S. A. Generalized vortex methods for free-surface flow problems // Journal of Fluid Mechanics. 1982. Vol. 123. P. 477–501.
- [42] Lamb H. Hydrodynamics. Cambridge, UK: Cambridge University Press, 1932. 738 p.
- [43] Cottet G.-H., Koumoutsakos P. D. Vortex methods: theory and practice. Cambridge, UK: Cambridge University Press, 2000. 313 p.
- [44] Gorban I. M., Khomenko O. V. Flow control near a square prism with the help of frontal flat plates // Studies in Systems, Decision and Control. Cham, Germany: Springer International Publishing, 2016. P. 327–350.
- [45] Gorban I. M., Lebid O. G. Numerical modeling of the wing aerodynamics at angle-of-attack at low Reynolds numbers // Modern Mathematics and Mechanics. Cham, Germany: Springer International Publishing, 2018. P. 159–179.
- [46] Clamond D., Dutykh D. Fast accurate computation of the fully nonlinear solitary surface gravity waves // Computers & Fluids. 2013. Vol. 84. P. 35–38.
- [47] Котельнікова А. С., Нікішов В. І., Срібнюк С. М. Взаємодія поверхневих поодиноких хвиль з підводними перешкодами // Доповіді Національної академії наук України. 2012. № 7. С. 54–59.
- [48] Byatt-Smith J. G. B. An integral equation for unsteady surface waves and a comment on the Boussinesq equation // Journal of Fluid Mechanics. 1971. Vol. 49, no. 4. P. 625–633.
- [49] Chan R. K.-C., Street R. L. A computer study of finite-amplitude water waves // Journal of Computational Physics. 1970. Vol. 6, no. 1. P. 68–94.
- [50] Maxworthy T. Experiments on collisions between solitary waves // Journal of Fluid Mechanics. 1976. Vol. 76, no. 1. P. 177–186.
- [51] Lo D., Young D. Arbitrary Lagrangian–Eulerian finite element analysis of free surface flow using a velocity-vorticity formulation // Journal of Computational Physics.—2004.—Vol. 195, no. 1.—P. 175–201.
- [52] Li Y., Raichlen F. Energy balance model for breaking solitary wave runup // Journal of Waterway, Port, Coastal, and Ocean Engineering. 2003. Vol. 129, no. 2. P. 47–59.

## І. М. Горбань, А. С. Корольова, В. А. Воскобійник, В. М. Вовк Динаміка солітонної хвилі та вихрові поля навколо занурених щілинних бар'єрів

Захист прибережних територій штучними спорудами є актуальною проблемою для спільноти, що займається береговою технічною інфраструктурою. У цьому дослідженні для зменшення висоти й енергії хвиль пропонується використовувати вертикальний занурений екран з горизонтальними щілинами. Зустрічаючи таку перешкоду, падаюча хвиля розпадається на прохідну та відбиту. Окрім того, через відрив потоку зі стінок споруди частина хвильової енергії перетворюється на кінетичну енергію вихрового поля. Дослідження зосереджено на оцінці гідравлічної якості цього хвилегасника, яка вимірюється коефіцієнтами відбиття й проходження хвилі. Також з метою отримання інформації про напрямки та інтенсивність водообмінних течій та про розмив донної поверхні розглядаються циркуляційні процеси навколо споруди. Задача аналізується у вертикальній площині, де конструкція має вигляд щілинного бар'єра. Передбачається, що бар'єр складається з трьох непроникних елементів і, залежно від розташування нижнього елемента відносно дна, приймає одну з двох можливих конфігурацій: нижня секція лежить на дні, або між бар'єром і морським дном є щілина. Для визначення найбільш ефективної конструктивної схеми такого хвилегасника виконано чисельне дослідження взаємодії солітонної хвилі зі щілинними бар'єрами різної форми та проникності. Розвинена обчислювальна процедура поєднує метод граничних інтегральних рівнянь, який використовується для визначення деформацій вільної поверхні, й гібридну вихрову схему для моделювання вихрового поля, породженого хвилею. Достовірність методики перевірено шляхом порівняння отриманих результатів з даними фізичного експерименту, проведеного в експериментальному каналі Інституту гідромеханіки НАНУ, а також із результатами інших авторів. Амплітуда розглянутої солітонної хвилі складала  $A_i/h = 0.2$ . Аналіз еволюції вільної поверхні, а також енергетичних коефіцієнтів відбиття й проходження показав, що захисні властивості щілинного бар'єра погіршуються зі збільшенням його проникності. Разом з тим, вплив ефекту проникності сильніший для високих та вузьких бар'єрів, ніж для низьких і широких. Дослідження вихрового поля, яке генерується солітонною хвилею навколо щілинного бар'єра, виявило складну картину течії з підвітряного боку споруди. Тут утворюються дві вихрові пари з протилежно спрямованих структур, взаємодія яких формує низхідний і висхідний потоки води вздовж бар'єра. Також ці вихори виштовхують рідину крізь щілини до навітряного боку споруди, завдяки чому утворюється зворотний потік води між прибережною зоною та відкритим морем. Завдяки цьому інтенсивність водообміну між різними боками конструкції збільшується на порядок, у порівнянні з непроникним бар'єром. Отримані дані свідчать про те, що щілинний бар'єр із пористістю (0.2...0.3) буде найбільш вдалим серед конструкцій цього типу як з точки зору берегозахисту, так і для збереження екології в прибережній зоні.

КЛЮЧОВІ СЛОВА: солітонна хвиля, занурений хвилегасник, бар'єр з горизонтальними щілинами, метод граничних інтегральних рівнянь, вихровий метод